Structure and Properties of Partially Neutralized Poly(acrylic acid) Gels

F. Schosseler,† F. Ilmain,‡ and S. J. Candau*,‡

Institut Charles Sadron, CRM-EAHP, 6 rue Boussingault, 67083 Strasbourg Cedex, France, and Laboratoire de Spectrométrie et d'Imagerie Ultrasonores, Unité de Recherche Associée au CNRS No. 851, Université Louis Pasteur, 4 rue Blaise Pascal, 67070 Strasbourg Cedex, France

Received January 27, 1990; Revised Manuscript Received May 25, 1990

ABSTRACT: The compressional osmotic and shear moduli, the static structure factor, and the cooperative diffusion constant of partially neutralized poly(acrylic acid) gels have been measured in the reaction bath as a function of polymer concentration, ionization degree, salt concentration, and cross-linking degree. The variations of the compressional modulus with these parameters are in good agreement with those predicted from simple theoretical arguments. The structure factor obtained from small-angle neutron scattering exhibits a peak, in a limited range of ionization degree and salt concentration. The variations of the amplitude and the position of the peak as a function of the ionization degree, for a given polymer concentration, are reasonably described by a recent theoretical model developed for a semidilute solution of weakly charged polymers in a poor solvent. From the measurements of the cooperative diffusion coefficient, it is inferred that the friction coefficient is an increasing function of the polymer concentration and ionization degree.

I. Introduction

A fundamental parameter in polyelectrolyte systems is the linear charge density of the polymer chains.[1-8] For highly charged polymers, the distance between two ionizable groups on the chain is smaller than the Bjerrum length, and, due to counterion condensation,[9] the linear charge density is thought to be independent of the amount of ionizable groups. This corresponds to the strong electrostatic coupling limit where the electrostatic forces overcome the monomer-monomer interactions.[1,2,4-6] On the other hand, for weakly charged chains, the ionizable groups are well separated on the chains and a small variation of the ionization degree modifies strongly the properties of the system. Excluded-volume effects can play an important role in this weak coupling limit.[3,7,8]

Fully sulfonated poly(sodium sulfonate styrene) (NaPSS) is a typical example of a highly charged polyelectrolyte. Solutions of NaPSS in pure or salted water have been studied by using small-angle neutron (SANS)[10] or X-ray (SAXS)[11] scattering, quasi-elastic light (QELS)[12] or neutron (NSE)[13] scattering, osmometry,[14] and viscometry.[15]

Partially neutralized poly(methacrylic acid) (PMA)[16] or poly(acrylic acid) (PAA)[17-20] are good examples of weakly charged chains. The ionization degree of these polymers can be continuously varied from zero to one, thus providing a convenient way to progressively increase the electrostatic coupling. Several studies using scattering techniques[16,17,19,20] have reported on the effect of the ionization degree on the local conformation or the radius of gyration of polyelectrolyte chains.

In the weak coupling limit, solutions of polyelectrolytes might exhibit complex structure due to the hydrophobic character of the backbone. In that case the solubilization is ensured by the electric charges. This effect, pointed out already 15 years ago,[1,21] was clearly demonstrated in swelling experiments performed on ionic gels swollen in poor solvents.[22]

More recently the problem of weakly charged polyelectrolytes in a poor solvent received more attention.[7,8] It was argued that systems, where attractive dispersion forces are nearly compensated by repulsive electrostatic interactions, should undergo a microphase-separation transition. The phase separation occurs on a microscopic scale because a macroscopic phase separation would result in a too severe loss of entropy for the counterions.

Thus, the physics underlying the properties of a polyelectrolyte system depends on the range of ionization degree. Although this appears to be a very difficult theoretical problem, it is of considerable practical use. For example, the intrinsic properties of superabsorbant gels (gels with high water retention capacity) can be optimized through the combined variation of their ionization and cross-linking degrees.[23]

In this paper we report on an experimental study of partially neutralized poly(acrylic acid) gels. The acrylic monomers are neutralized by sodium hydroxide prior to polymerization and the fraction of neutralized monomers is varied between 0 and 0.8. The gels are studied at the concentration at which they are prepared. The concentration in the reaction bath has been varied between 30 g/L (0.416 M) and 150 g/L (2.08 M). The effects of added salt are also described. Following the experimental section, part III describes the results obtained by SANS experiments and gives the variations of compressional modulus, shear modulus, and cooperative diffusion coefficient with polymer concentration and ionization degree. In the discussion we try to sum up the results in an overall qualitative picture of the evolution of the gel structure when the ionization degree is varied.

II. Experimental Section

1. Sample Preparation. Gels were prepared by radical copolymerization in an aqueous solution of acrylic acid and *N,N'*-methylenebis(acrylamide). The gelation reaction is initiated by ammonium peroxydisulfate and performed in an oven at 70 °C. The ionization degree, α, is defined as the ratio of the number of carboxylate groups to the total number of monomers. Since poly(acrylic acid) is a weak acid, α can be varied over a wide range by changing the pH of the medium. In aqueous solution, α has a nonzero value due to the acido-basic equilibrium:

$$-CH_2CH(COOH)- + H_2O \overset{K_a}{\rightleftharpoons} -CH_2CH(COO^-)- + H_3O^+ \quad (1)$$

The ionization degree is a decreasing function of the polymer concentration. For the concentrations used in this study (0.416

† Institut Charles Sadron.
‡ Université Louis Pasteur.

0024-9297/91/2224-0225$02.50/0

$M < C_p < 2.08$ M), the dissociation of the polyacid is very low. Thus, we have approximated the dissociation constant to that of the monomeric acrylic acid: $K_a = 5.6 \times 10^{-5}$. This leads to values of α decreasing from 1.2×10^{-2} to 5×10^{-3} when the polymer concentration increases from 0.416 to 2.08 M.

Higher ionization degrees ($\alpha > 10^{-2}$) were obtained by partial neutralization of the polyacid with NaOH to a given stoichiometric ionization degree according to

$$-CH_2CH(COOH)- + Na^+OH^- \rightarrow -CH_2CH(COO^-) + H_2O + Na^+ \quad (2)$$

Very low ionization degrees ($\alpha < 5 \times 10^{-3}$) were obtained by addition of HCl to the solution to shift the dissociation equilibrium of the weak acid toward the acidic form:

$$-CH_2CH(COO^-)- + H_3O^+ + Cl^- \overset{K_a}{\rightleftarrows} -CH_2CH(COOH)- + H_2O \quad (3)$$

In the following, we will distinguish between f, the stoichiometric neutralization degree, and α, the effective ionization degree. The actual fraction of ionized monomers α is calculated by taking into account the fraction of monomers neutralized by NaOH f and the fraction of autodissociated monomers. For high f values ($f > 0.1$) the two quantities can be considered as equal with a good approximation.

Gels were prepared either by weighing all the components or by adding to mixtures of monomer, cross-linking agent, ammonium peroxydisulfate, and the desired amount of sodium hydroxide the amount of water required to complete a given total volume of solution. In the first method we have calculated the concentrations using for the partial molar volumes of acrylic acid and sodium hydroxide $V_{AA} = 62.4$ cm^3 mol^{-1} and $V_{NaOH} = -5.2$ cm^3 mol^{-1}.[24] We have neglected the contributions of the N,N'-methylenebis(acrylamide) and the ammonium peroxydisulfate to the total volume. A typical composition is 10 g of acrylic acid, 0.1 g of N,N'-methylenebis(acrylamide), and 33 mg of peroxydisulfate in 90 g of water. As the partial molar volume of poly(acrylic acid) is smaller than that of the monomer ($V_{PAA} = 45.4$ cm^3 mol^{-1}),[24] we corrected the concentration of the final gels to account for this effect by assuming a complete conversion of the monomer. This correction is smaller than 4% for the most concentrated samples. After the components were mixed, the solutions were filtered with 0.2-μm filters to get rid of dust particles. Gelification was carried out at 70 °C during 12 h directly in the scattering cell after nitrogen has been bubbled in the solution to remove the dissolved oxygen that would inhibit the radical reaction. Samples for SANS experiments were prepared along the same lines but with replacement of H_2O by D_2O to obtain a good contrast. The samples prepared at the lowest polymer concentration, i.e., $C_p = 0.42$ M, were not macroscopic gels but solutions of branched polymers. The results of the SANS study performed on these samples were discussed together with those obtained from macroscopic gels.

2. SANS Experiments. Three different sets of experiments were performed on spectrometer PACE in Laboratoire Léon Brillouin (Laboratoire commun CEA–CNRS). For each set we used two different apparatus configurations in order to cover a wide range of scattering vectors q ($5 \times 10^{-3} \lesssim q$ (Å^{-1}) $\lesssim 0.15$). In the first and second experiments, we kept the sample–detector distance equal to 3.00 m and used two different wavelengths for the incident neutrons, $\lambda = 5.04$ Å and $\lambda = 14.86$ Å. In the last experiment, the wavelength was kept to 8 Å, and the sample detector distance was 1.50 or 4.50 m.

All data were treated according to standard procedures for small-angle isotropic scattering. The spectra were corrected for absorption, sample thickness, and electronic noise.

Solutions with the same compositions as those used to prepare gels were taken as background samples, except for the first set of experiments, where they did not contain cross-linking agent. This introduces no differences in the background samples since the total incoherent scattering of N,N'-methylenebis(acrylamide) molecules is negligible compared to that of the acrylic acid monomers.

Normalization to the unit incident flux, geometrical factors, and detector cell efficiency corrections were performed by using the incoherent scattering of H_2O, corrected for the scattering of the empty cell. The data were put on an absolute scale by introducing the differential cross section per unit volume of H_2O at 25 °C.[25] This method gave a good matching of the spectra from the two different configurations used in the first experiment. However, in the second experiment, performed with the same configurations, we had to use a correcting factor 15% larger than the calculated one to get a satisfactory matching of the data. This disagreement could be due to a different ambient temperature in the experimental hall during the two sets of experiments. In the third experiment, the matching of the two different configurations is directly obtained from the normalization by H_2O spectra measured at the two different detector–sample distances.

3. Light-Scattering Experiments. The optical source on the light-scattering apparatus is a Spectra-Physics argon ion laser operating at $\lambda_0 = 4880$ Å. The time-dependent correlation function of the scattered intensity is obtained by using a 64-channel digital correlator (Brookhaven BI 2030). The Amtec goniometer allows us to vary the scattering angle between 10° and 160°.

For all the gels investigated in this study the intensity correlation data have been processed by using the method of cumulants to obtain the average decay rate, $\langle\Gamma\rangle$, and the variance, $\upsilon = (\langle\Gamma^2\rangle - \langle\Gamma\rangle^2)/\langle\Gamma^2\rangle)$. We did not observe intensity correlation functions with two distinct decay rates,[26,27] as has been reported for polyelectrolyte solutions,[12] but rather a moderate distribution of exponential decays ($\upsilon \leq 0.1$). We have verified that, for poly(acrylic acid) solutions ($M_w = 150\,000$), in the same range of concentration and zero neutralization degree, the intensity correlation function shows two modes. Thus, the analysis of the correlation function is easier for gels than for solutions. However, in doing such an analysis, one must take into account the fact that the intensity scattered from longitudinal fluctuations of swollen networks is generally heterodyned to some extent by the quasi-static component due to nonrandom, long-range, stationary concentration fluctuations.[28] These microscopic swelling inhomogeneities in the gel may produce an error in the determination of the flat background, B, of the autocorrelation function. Therefore, we have considered B as a fitting parameter in our data analysis. Deviations of the fitted value from the value computed by the correlator ranged from 0.2% to 1.5%.

In order to check whether the scattered signal is fully heterodyned, we measured the autocorrelation function obtained by mixing the scattered signal with an external oscillator using a Michelson-type interferometer. The comparison between the results obtained with and without reference beam has been discussed in a previous paper.[26] It has been shown that, for small scattering angles, the time-dependent term is fully heterodyned by the static scattering, while, for large scattering angles, the measured signal corresponds to a homodyne detection.

The above-mentioned static scattering usually prevents the measurements of the scattered intensity from the dynamic concentration fluctuations of gels. However, at large scattering angle, since the scattering regime is very close to a pure homodyne one, the contribution from static scattering is small. Therefore, we have performed the light-scattering intensity measurements at a scattering angle of 90° ($q = 2.42 \times 10^{-3}$ Å^{-1}) without correction for the static scattering from heterogeneities. It must be added that very recent experiments performed on large samples of ionized gels showed no angular dependence of the scattered intensity and a pure homodyne behavior in the 25–140° range of scattering angles. The behavior of scattered intensity as a function of ionization degree and of salt content is the same as that reported here.[29]

4. Shear Modulus Measurements. The shear modulus can be obtained in a uniaxial compression experiment if the volume of the sample is kept constant. In practice, for gels this is achieved by performing the measurement in a time shorter than the characteristic deswelling time of the gels. In the experimental setup used in this study, the cylindrical gel is compressed by a piston attached to a calibrated force sensor. The displacements of the piston are controlled through a micrometric screw. For each displacement, the corresponding force, g, is measured. For neutral swollen gels, the plot of $g/S/(\lambda' - 1/\lambda'^2)$ vs $1/\lambda'$ gives

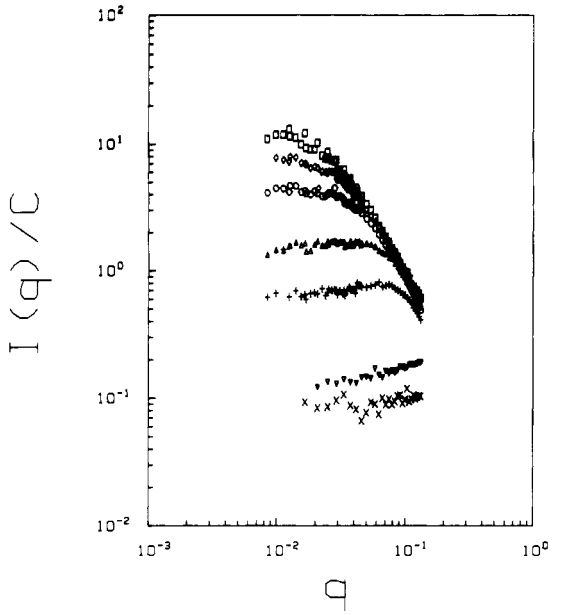

Figure 1. Intensity scattered by gels with different ionization degrees and the same polymer concentration, C_p = 1.44 M (logarithmic scales): (□) α = 0.006; (◇) 0.013; (○) 0.022; (△) 0.051; (+) 0.1; (▽) 0.4; (×) 0.8.

usually horizontal straight lines. Here S is the surface of the undeformed gel and λ' is the elongation ratio of the gel. The plateau value in this representation corresponds to the value of the shear modulus, μ. Horizontal straight lines are also obtained in the above representation for the ionized gels, which allows one to determine with a good accuracy the shear modulus. Values of λ' during the experiment are typically between 1 and 0.8.

III. Experimental Results

1. SANS Experiments. Typical scattering curves are shown in Figure 1. As a constant and general trend, one observes a decrease of the scattering intensity when the ionization degree is increased.

At first sight, the systems can be divided into two series, depending on the range of ionization degree.

For small neutralization degrees ($f < 0.1$), the intensity scattered at high q values is independent of the value of f and decreases as q^{-a}, with $1.7 \leq a \leq 2.1$. At smaller q values, the structure factor seems to reach a plateau value that becomes lower as the ionization degree increases.

For higher neutralization degrees ($f > 0.1$), experiments become very difficult because the scattered intensity is very weak and the standard error is rather large. In the investigated q range, the scattered intensity increases steadily with the value of the scattering vector.

From the data of Figure 1, one could guess that all samples exhibit the same general behavior in the high q range ($0.1 < q$ (Å^{-1}) < 0.5), i.e., the scattered intensity being a decreasing function of q. This would correspond to a maximum around $q \sim 0.2$ Å^{-1} in the intensity scattered from the highly charged samples. The existence of such a maximum in the scattered intensity has been reported[10] for salt-free NaPSS solutions. The expected position of this hypothetical maximum in the scattering curves of Figure 1 would be consistent with the well-known $C_p^{1/2}$ dependence of the peak position in NaPSS systems.[1,4-6,10] Here, C_p is the molar concentration in monomers.

A closer examination of Figure 1 suggests that the intensity scattered by the sample with f = 0.1 exhibits a smeared maximum. The presence of a peak appears more clearly in samples with smaller polymer concentration and neutralization degrees, as shown on Figure 2. Figure 3

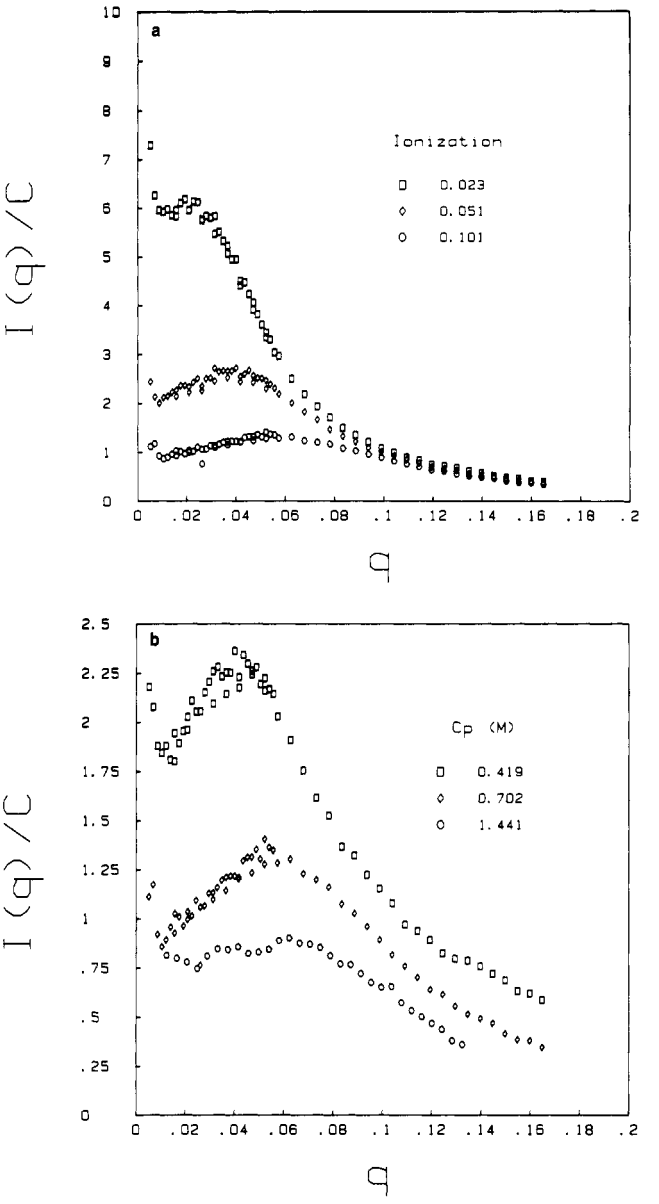

Figure 2. Plot on linear scales of the intensity scattered by gels with (a) different ionization degrees and the same polymer concentration, C_p = 0.707 M, and (b) the same ionization degree, $\alpha \simeq 0.1$, and different polymer concentrations.

summarizes the experimental conditions (concentration and ionization degree) where the peak can be observed within the q range allowed by the SANS technique.

The decrease of the neutralization degree induces a shift of the peak position to smaller q values (Figure 2a). Decreasing the polymer concentration has the same but much weaker effect (Figure 2b). It must also be noted that the structure factor of the most diluted sample (C_p = 0.42 M), which corresponds to a solution of highly branched polymers (cf. the Experimental Section), does not differ qualitatively from those of the macroscopic gels obtained at higher polymer concentrations. The positions and heights of the maxima are listed in Table I.

Turning now to the high q regime, one must recall first that, for polymer systems above the overlap concentration, C^*, the intermediate scattering regime corresponds to q^{-1} values in between the monomer size and the blob size.[31] In this regime, the intensity, $I(q)$, should be proportional to the monomer concentration, C, and $I(q)/C$ should be independent of the concentration. Clearly, this is not the case in our experiments. If we consider samples with

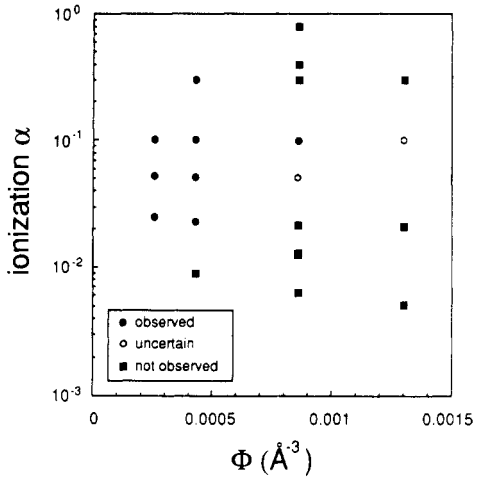

Figure 3. Observability of the peak in the q range allowed by the SANS technique as a function of polymer concentration and ionization degree. Φ is the number of monomers per unit volume (in angstroms cubed).

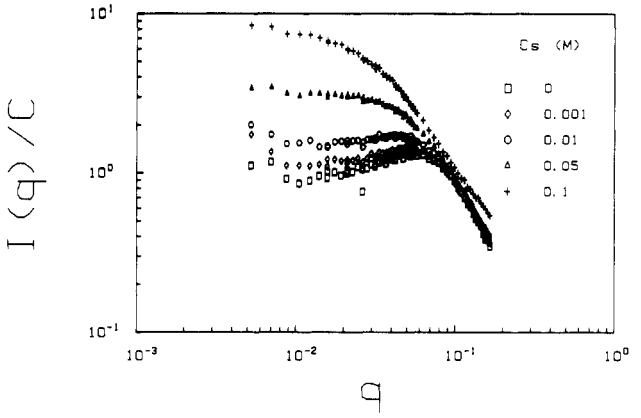

Figure 4. Evolution of the scattering intensity with the amount of added NaBr. C_p = 0.707 M; α = 0.101.

neutralization degrees smaller than 0.3, the scattering curves coincide at high q values for a given polymer concentration (Figures 1 and 2a), but this is not true for samples with the same neutralization degree and different concentrations (Figure 2b). These observations suggest that, for these highly concentrated samples, the true asymptotic regime cannot be reached. Thus, the values of the exponent a in Table I are not simply related to the local conformation of the polymer chains.

We cannot exclude a possible variation of the scattering length density of the polymer due to complicated solvation effects for high polymer concentration. This would explain the increasing shift of the scattering curves when increasing the polymer concentration. This effect would not prevent us from measuring the peak position. However it would affect the absolute values of the scattering intensity by numerical factors that can be determined by forcing the superposition of the curves in the high q range. As a matter of fact, it appears that, by taking into account these numerical factors, one improves the agreement between the experimental peak intensities and the predictions of the theoretical model.

Finally, it must be mentioned that, in the case of polyelectrolytes systems, it is no longer allowed to neglect the intensity scattered by the counterions for $C_p \simeq 1.4$ M, when $f \geq 0.4$ and $q > 0.1$ Å.[32]

The influence of added salt on the scattering intensity is shown in Figure 4. The addition of NaBr does not change the intensity scattered at high q values. On the other hand, the peak position shifts to smaller q values and its amplitude increases as the concentration of added salt increases. Finally, the peak disappears while the intensity at zero q value increases as the salt concentration is further increased.

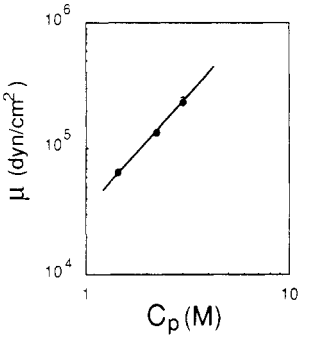

Figure 5. Variation of the shear modulus with the polymer concentration for gels with a neutralization degree equal to zero. The cross-linking degree is kept to $R = 4.7 \times 10^{-3}$.

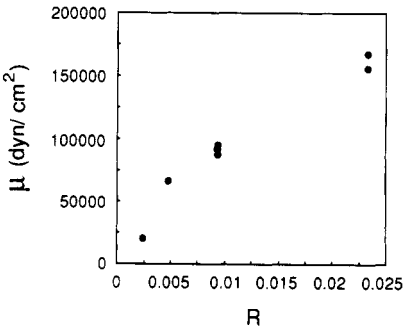

Figure 6. Variation of the shear modulus with the cross-linking degree, R, defined as the ratio of molar bis(acrylamide) to molar acrylic acid concentration. The neutralization degree is zero, and the polymer concentration is C_p = 1.44 M.

2. Elastic Moduli. Shear Modulus. The variation of the shear modulus as a function of the polymer concentration in the reaction bath is shown on Figure 5 for gels with no neutralization. The ratio bis(acrylamide)/acrylic acid is kept constant. It was not possible to measure the shear modulus of gels with smaller concentrations because these gels are too sticky to be easily handled. On this limited concentration range, it is possible to describe the data with an empirical power law $\mu \sim C_p^x$ where $x \simeq 1.8$ (Figure 5). Even though no definite conclusion can be drawn from this limited amount of raw data, it is worthwhile to point out that such a dependence of the shear modulus on the concentration of preparation is much stronger than the linear dependence predicted by the classical theory of rubber elasticity.[33] Clearly, these results show that the molecular weight of elastically effective chains does not remain constant as the polymer concentration is increased. In fact, it is well-known that, in a radical-type reaction, the amount of disproportionation or termination reactions depends on the concentration in the reaction bath. This parameter is also known to be implied in the formation of the number of trapped entanglements.[34] Furthermore, several studies have shown that the radical copolymerization leads to a nonrandom cross-linking that generates inhomogeneities in the gel.[28] Thus, the combined effects of dangling ends, loops, trapped entanglements, and nonrandom cross-linking are likely to be at the origin of the behavior observed in Figure 5.

Figure 6 shows the influence of the cross-linking degree on the shear modulus, for a polymer concentration C = 0.1 g/cm^3 and a neutralization degree f = 0. Under these

Table I
Characteristics of the Samples Studied by SANS

sample	C_p, M	α	C_s, M	exponent a	10^2q, Å^{-1}	$10^2I(q^*)$	κ^{-1}, Å	A (Å$^{-1/2}$) = $(q^{*2}+\kappa^2)/\alpha\Phi^{1/2}$
				April 1988				
G1000	1.441	0.006	0	1.77 ± 0.02			46	
G1001	1.441	0.013	0	1.7 Ω 0.02			32	
G1002	1.441	0.022	0	1.83 ± 0.03			24	
G1005	1.442	0.051	0	1.59 ± 0.04			16	
G1010	1.442	0.100	0	1.58 ± 0.04	6.12 ± 1.90	8.0 ± 2.0	11	3.90 ± 0.90
G1040	1.445	0.400	0				6	
G1080	1.450	0.800	0				6	
				January 1989				
G500	0.707	0.009	0	2.02 ± 0.03			54	
G502	0.707	0.023	0	2.01 ± 0.03	1.98 ± 0.45	35.4 ± 3.0	34	2.66 ± 0.43
G510(1)	0.707	0.101	0	1.83 ± 0.06	5.59 ± 0.99	7.2 ± 1.9	16	3.35 ± 0.61
G530	0.708	0.300	0		8.68 ± 1.73	2.2 ± 0.8	9	3.06 ± 0.55
G1000	1.441	0.006	0	2.23 ± 0.05			46	
G1002	1.441	0.022	0	2.28 ± 0.05			24	
G1010	1.442	0.100	0	1.84 ± 0.12	6.27 ± 2.34	9.2 ± 7.8	11	3.96 ± 1.11
1030	1.444	0.300	0				7	
G1500	2.204	0.005	0	1.98 ± 0.04			41	
G1502	2.204	0.021	0	2.07 ± 0.06			20	
G1510	2.207	0.100	0	1.47 ± 0.09	4.60 ± 1.43	10.9 ± 1.4	9	3.83 ± 0.5
G1530	2.212	0.300	0				5	
				June 1989				
G32	0.419	0.025	0	1.79 ± 0.01	1.86 ± 0.37	23.3 ± 2.6	42	2.29 ± 0.39
G35	0.419	0.052	0	1.38 ± 0.02	3.20 ± 0.23	11.0 ± 0.7	29	2.65 ± 0.22
G310	0.419	0.101	0	1.23 ± 0.02	3.99 ± 0.49	6.8 ± 0.7	21	2.41 ± 0.29
G52	0.702	0.023	0	1.82 ± 0.02	1.96 ± 0.51	30.7 ± 3.6	34	2.63 ± 0.48
G55	0.702	0.051	0	1.83 ± 0.03	3.69 ± 0.56	13.1 ± 1.6	23	3.12 ± 0.46
G510(2)	0.702	0.101	0	1.85 ± 0.04	5.55 ± 1.38	6.7 ± 2.5	16	3.32 ± 0.81
G510-3	0.702	0.101	0.001	1.6 ± 0.04	5.06 ± 0.95	7.1 ± 1.8	16	3.12 ± 0.53
G510-2	0.702	0.101	0.01	1.7 ± 0.04	4.21 ± 0.98	8.6 ± 2.2	14	3.21 ± 0.47
G5105-2	0.702	0.101	0.05	1.66 ± 0.03			10	
G510-1	0.702	0.101	0.1	1.41 ± 0.01			8	

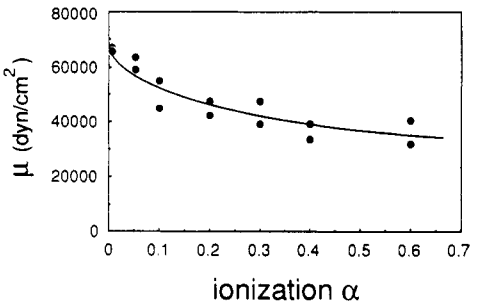

Figure 7. Variation of the shear modulus with the ionization degree. The cross-linking degree is $R = 4.7 \times 10^{-3}$, and the polymer concentration is equal to 1.44 M.

conditions the ionization degree can be estimated to be around 6.5×10^{-3}. Again, the simplest theory predicts that the shear modulus is proportional to the concentration of elastic chains. At constant polymer concentration, this leads to a proportionality between the shear modulus and the cross-linking degree. Clearly, this simple assumption cannot explain the data in Figure 6. Here, we do not want to elucidate this difficult problem, but we just want to underline the fact that a variation of the polymer concentration and/or the cross-linking degree produces a complex change of the network structure.

Figure 7 shows the dependence of the shear modulus on the ionization degree, α. For each α value, the two points correspond to measurements on two different cylindrical pieces of the same gel. It appears that results are more difficult to reproduce when the neutralization degree is nonzero. In fact, for samples with no neutralization, the same procedure has given couples of values that are not distinguishable on the scale of Figures 5 and 6. In spite of the scattering of the data, we observe that the introduction of charges reduces weakly the shear modulus of the gels. We have no explanation for this behavior. Even the very fact that charges affect the shear modulus is a priori a quite new and surprising result. It has to be noted that the same result is obtained if the gel is neutralized after the copolymerization reaction is completed. Thus the observed behavior seems to be related to the existence of charges in the gel and not to a possible chemical effect due to the presence of charges during the reaction.

Compressional Osmotic Modulus. A theory of light scattering from concentration fluctuations in gels has been given by Tanaka, Hocker, and Benedek.[35] These authors show that the time-correlation function of concentration fluctuations in the gel is inversely proportional to the longitudinal modulus, $M = K_{os} + (4/3)\mu$, where K_{os}, the compressional osmotic modulus, is defined as the inverse of the osmotic compressibility, $K_{os} = C\,\partial\pi/\partial C$, where π is the osmotic pressure. In the limit $q = 0$, the excess intensity scattered from concentration fluctuations in the gel is given by

$$\Delta I(q\to 0) = A_0 k_B T \left(\frac{dn}{dC}\right)^2 \frac{C^2}{M} \tag{4}$$

where k_BT is the thermal energy and dn/dC is the increment of refractive index with the polymer concentration C (in grams per cubic centimeter).

The absolute value of the longitudinal modulus can be obtained if we know the apparatus constant, A_0. From standard textbooks on light scattering,[36] one has for vertically polarized incident light and at a scattering angle of $\pi/2$

$$A_0 = \frac{4\pi^2}{\lambda_0^4} n_{ref}^2 \frac{I_{ref}(\pi/2)}{R_{ref}(\pi/2)} \tag{5}$$

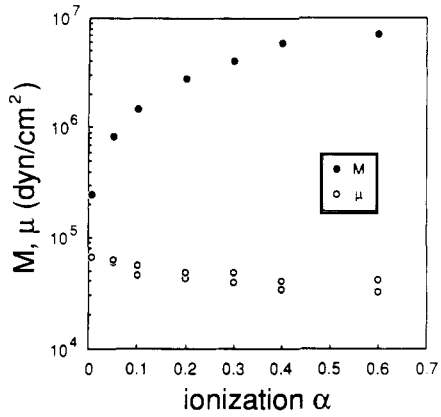

Figure 8. Evolution of the longitudinal modulus and of the shear modulus with the ionization degree (C_p = 1.44 M).

Here, $I_{ref}(\pi/2)$, $R_{ref}(\pi/2)$, and n_{ref} are, respectively, the scattering intensity at $\pi/2$ angle, the Rayleigh ratio, and the refractive index of a reference sample. In our case the reference is benzene. The values of the refractive index and of the Rayleigh ratio have not been measured for λ_0 = 4880 Å, and we have calculated them by interpolation, using the known values at λ_0 = 4360, 5460, and 6328 Å. We have found $n_{ref} \simeq 1.510$ and $R_{ref}(\pi/2) \simeq 4 \times 10^{-5}$ cm^{-1}. We have measured $I_{ref}(\pi/2) = 178.6$ in our arbitrary units. This leads to $A_0 \simeq 7.1 \times 10^{25}$ au/cm^3.

Kitano et al.[19] have measured the quantity dn/dC for dilute solutions of poly(acrylic acid) in water. They have found that dn/dC increases linearly from 0.12 to 0.18 as the neutralization degree increases from 0.1 to 1 in low ionic strength solutions. We were not able to measure the refractive index increment in our systems, and we assumed that the values obtained in dilute solutions did not change at higher concentration. We used $dn/dC \simeq 0.115 + 0.068f$, as estimated from the data in ref 19.

The striking effect of coulombic interactions on elastic moduli is illustrated in Figure 8: the introduction of charges into a gel reduces slightly the shear modulus but enhances strongly the longitudinal modulus as a result of the osmotic contribution of the free counterions. The data in Figure 8 allow one to extrapolate the values of the elastic moduli to zero ionization degree. One obtains for the longitudinal modulus $M = 2.5 \times 10^5$ dyn/cm^2 and for the shear modulus $\mu = 6.7 \times 10^4$ dyn/cm^2. Therefore, the extrapolated values $K_{os,n}$ and μ are of the same order of magnitude as for usual neutral gels.

In the limit of small ionization degrees, we can split the longitudinal modulus into three contributions, writing

$$M = K_{os,n} + K_{os,e} + (4/3)\mu \quad (6)$$

where $K_{os,n}$ and $K_{os,e}$ are the compressional osmotic modulus due, respectively to the neutral polymer network and to the free counterions and μ is the shear modulus of the neutral network. The contribution of charges to μ is neglected here since it is small (see Figure 7). In fact, the free counterions contribution, $K_{os,e}$, is much larger than the neutral network contribution, as shown in Figure 8. The osmotic pressure, π_e, associated with the free counterions is simply[1,37,38]

$$\pi_e = k_B T \Phi \alpha \quad (7)$$

where Φ is the number of monomers per unit volume and α the ionization degree. Using the definition of the compressional osmotic modulus, we obtain the same expression for $K_{os,e}$.

Thus, if we neglect the neutral network contribution in (6) and replace M by $K_{os,e}$ in (4), we find that the excess

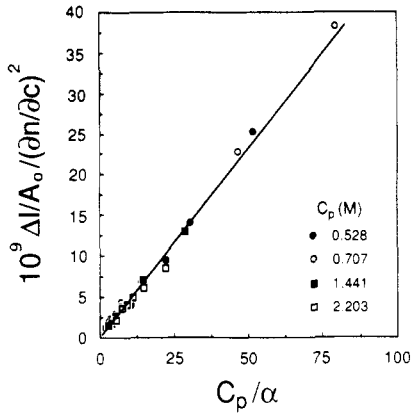

Figure 9. Plot of the normalized intensity (see text) scattered at $q = 2.42 \times 10^{-3}$ Å^{-1} as a function of C_p/α.

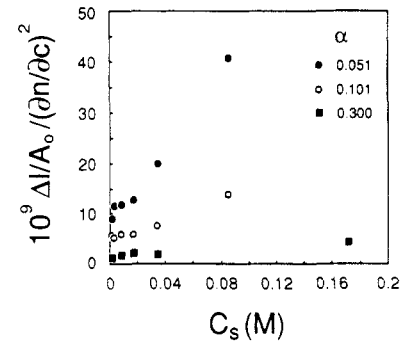

Figure 10. Scattered intensity ($q = 2.42 \times 10^{-3}$ Å^{-1}) as a function of salt concentration for different ionization degrees. The polymer concentration is kept to C_p = 0.707 M.

scattering intensity corrected by the proper dn/dC factor should be proportional to the ratio C_p/α.[27] This is observed quite nicely in Figure 9, where points corresponding to samples with four different polymer concentrations and varying neutralization degrees fall along the same line. This feature shows that $K_{os,e}$ gives the dominant contribution to M as soon as the ionization degree is larger than a few percent. However, as the polymer concentration increases, μ becomes larger (Figure 5) and this approximation needs higher ionization degrees ($\sim$0.1) to be valid.

Figure 10 shows the effect of added salt on the intensity scattered by gels with the same polymer concentration but different ionization degrees. This effect becomes more important as the ionization degree decreases. This is easy to understand qualitatively since the importance of salt effects should be related to the ratio of the Debye–Hückel length to the mean distance between charged monomers. The latter increases as the ionization degree decreases, while κ^{-1} is essentially fixed by the salt concentration. Thus, for a given salt concentration, the interactions between the well-separated charges of a weakly neutralized gel are completely screened. This is not true for highly charged samples near Manning's condensation threshold. Thus, we can expect that the ratio of the distance between two charges along the chain to the Debye–Hückel length, i.e., α^{-1}/κ^{-1}, will play an important role. Since $\kappa/\alpha \sim (\alpha C_p + 2C_s)^{1/2}/\alpha$, the simplest function that recovers the right behavior in the absence of salt is $\Delta I(C_s) \sim (\kappa/\alpha)^2$. The same result will be derived more rigorously in the discussion.

Cooperative Diffusion Coefficient. The variation of the cooperative diffusion coefficient, D_c, with the ionization degree is shown on Figure 11 for different polymer concentrations. As a general trend, the introduction of charges into the gels increases steadily the value of D_c for

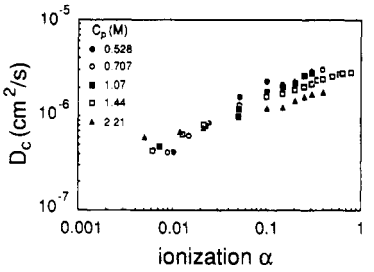

Figure 11. Variation of the cooperative diffusion coefficient with the ionization degree for different polymer concentrations.

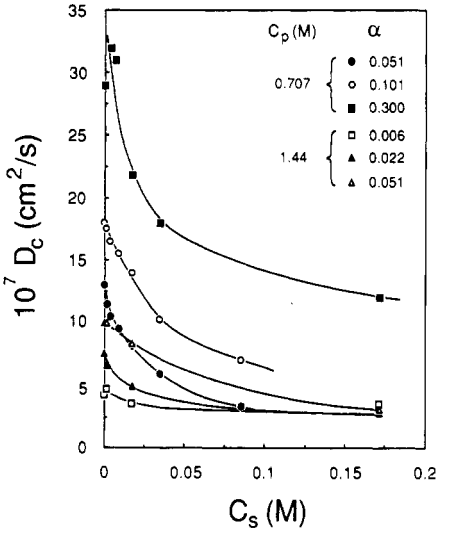

Figure 12. Influence of added salt (NaCl) on the cooperative diffusion coefficient for different polymer concentrations and ionization degrees.

a given concentration.[26] The curves corresponding to each polymer concentration are crossing each other for an ionization degree, α, of around 0.02. This means that, for $\alpha \simeq 0.02$, the cooperative diffusion coefficient is independent of the polymer concentration for the gels investigated here. This allows us to define two different regimes in Figure 11, depending on whether α is smaller or larger than 0.02. For small α values ($\alpha < 0.02$), coulombic interactions can be considered as a perturbation of the concentration fluctuations in the gel: typically for $\alpha \simeq 5 \times 10^{-3}$ and $C = 0.1$ g/cm^3, the contour distance on the chain between two charges ($\simeq$500 Å) is larger than that between two neighboring cross-links ($\simeq$250 Å). Thus, as in neutral gels, D_c increases with the polymer concentration.[27] When $\alpha \to 0$, the D_c (C) variation approaches that of nonionic gels.

For larger α values ($\alpha > 0.02$), the opposite behavior is observed: for a given ionization degree, the cooperative diffusion coefficient decreases when the polymer concentration increases. Nevertheless, it has been shown in a preceding paper[27] that the cooperative diffusion of these gels is insensitive to a variation of cross-linking degree for a given polymer concentration. In this respect, the gel behaves as a semidilute solution of long polymeric chains.

The salt effect is illustrated in Figure 12. It is seen that the addition of salt produces a large decrease in D_c for all the ionization degrees except the smaller ones. This behavior is the opposite of that observed for the scattered intensity, where the less charged samples were found to be the most sensitive to the addition of salt. Moreover, the addition of salt produces a larger decrease of the D_c value when the polymer concentration decreases. For the smallest ionization degrees, it seems that above a certain salt concentration, the cooperative diffusion coefficient becomes independent of the ionization degree and polymer concentration.

IV. Discussion

The most interesting feature of the SANS results is the presence for some systems of a peak in the structure factor (cf. Figure 3). The existence of a peak in the intensity scattered by a NaPAA solution with $f = 0.1$ was already mentioned 10 years ago.[17] The theoretical models developed for semidilute solutions of polyelectrolytes in the limit of strong coupling predict such a peak. The isotropic model proposed by de Gennes et al.[1] is based on the concept of the screening length, ξ, used in semidilute solutions of neutral polymers. At scale lower than ξ, the electrostatic interactions are important and result in a fully exerted excluded volume between monomers. Beyond ξ, the electrostatic interactions are screened by other chains and each chain is Gaussian at large scale. In this model the peak of $I(q)$ demonstrates the short-range order arising from the hard-sphere-like repulsion between blobs. Hayter et al.[13] proposed that each polyion creates a correlation hole of radius κ^{-1}, from which other polyions are expelled. The common feature of these models as well as of the scaling approaches developed by Odijk[2] is the $C_p^{1/2}$ dependence of q^*, the wave vector corresponding to the maximum of $I(q)$.

The weak coupling limit, i.e., the range where the contour length between two successive charges on the chain is larger than both the Bjerrum length and the Debye-Hückel length, has been considered by Pfeuty.[3] For long chains at concentrations just above the crossover concentration, C_p^*, and without added salt, the correlation length, ξ, varies with α and C_p according to

$$\xi \propto C_p^{-1/2}\alpha^{-1/3} \tag{8}$$

The above relation is obtained for the case where the effect of small ions can be ignored. As the polymer and/or salt concentration is increased, this effect cannot be neglected and, locally, the chains become successively swollen and then Gaussian.

More recently, a model has been proposed[7,8] for weakly charged polyions having an amphiphilic character, due to a poor solubility of the polymer backbone in water. According to this model, in the semidilute regime, these systems are liable to form mesophases consisting in polymer-dense and polymer-dilute regions arranged in a periodic array. Above the mesophase-separation transition, the structure factor, $S(q)$, has a peak at a finite wavevector q^* that fixes the period of the mesophase. The variations of q^* as a function of polymer concentration and ionization degree are given by

$$(q^{*2} + \kappa^2)^2 = \frac{24\pi l\Phi\alpha^2}{g'a^2} \tag{9}$$

where l is the Bjerrum length, a is the monomer size, and g' is a numerical factor equal to $^1/_2$ or $^1/_3$, depending on the value of $(Nq^{*2}a^2/6)$.

Equation[9] predicts that, upon increasing the polymer concentration and/or the ionization degree, the peak position moves to larger values of the wavevector. On the other hand, for given α and Φ values, the addition of salt increases κ^2 and the peak shifts to lower q values according to (9). When κ is larger than $(24\pi l\alpha^2\Phi/g'a^2)^{1/4}$, the peak disappears and $S(q)$ decays monotonically to zero.

When the polymer concentration is not too large and the salt concentration small compared to $\alpha\Phi$, the amplitude

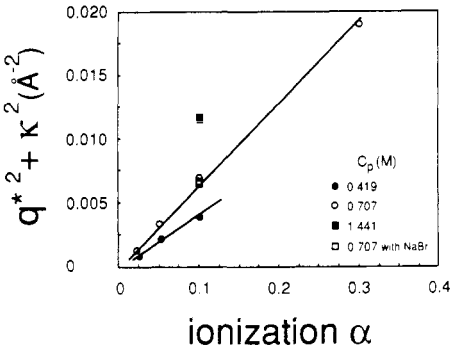

Figure 13. Plot of the quantity $q^{*2} + \kappa^2$ as a function of the ionization degree for different polymer concentrations. According to (9), this representation should give straight lines crossing the origin, with the slope proportional to $C_p^{1/2}$.

$S(q^*)$ of the peak can be approximated by[7,8]

$$S(q^*) \simeq (4\pi l)^{-1}\frac{q^{*2} + \kappa^2}{\alpha^2} \tag{10}$$

which can also be written by using eq 9:

$$S(q^*) \simeq (4\pi l)^{-1}\left(\frac{24\pi l}{g'a^2}\right)^{1/2}\frac{\Phi^{1/2}}{\alpha} \tag{11}$$

At first sight the above model is liable to describe the SANS spectra obtained in this study in the weak coupling range $0.02 \leq \alpha \leq 0.1$ where a peak is present.

The experimental results reported in Figures 1, 2, and 4 are in qualitative agreement with the predictions of (9) and (11). For instance, it can be seen that the position of the peak shifts toward lower values when the ionization degree or the polymer concentration is decreased. The addition of salt produces the same effect. In order to perform a quantitative comparison, we have calculated for different samples the ratio $(q^{*2} + \kappa^2)/(\alpha\Phi^{1/2})$, which, according to (9), should be a constant $A = (24\pi l/g'a^2)^{1/2}$. The results reported in Table I show that, for a given polymer concentration, $(q^{*2} + \kappa^2)/\alpha\Phi^{1/2}$ is in the first approximation independent of α and of C_s. However, one observes a slight increase of this quantity with the polymer concentration. Figure 13 shows the variation of $q^{*2} + \kappa^2$ as a function of the ionization degree for different polymer concentrations. According to (9), this representation should give straight lines passing through the origin. The agreement is quite good, in particular, for the gels with $C_p = 0.71$ M: points corresponding to samples in pure or salted water lie along the same line. On the other hand, the slopes of the straight lines are not proportional to $C_p^{1/2}$. It must also be noted that the calculated value of A, using $l = 7$ Å, $g' = 1/2$, and $a = 2.5$ Å, is $A = 13$ Å$^{-1/2}$. In fact, the above calculation does not take into account the natural persistence length, L_p, of the polymer that for PAA is $L_p \simeq 12$ Å. Replacing a^2 by $L_p a$ in the expression of A, one finds $A \simeq 8.2$ Å$^{-1/2}$, which is of the same order of magnitude as the experimental values.

Looking to the salt dependence for the series of gels, at concentration 0.71 M and ionization degree 0.1, and using the average experimental value $A = 3.1$ Å$^{-1/2}$, one finds that the peak should disappear for $\kappa > 0.08$ Å^{-1}. This corresponds to a salt concentration $C_s = 0.025$ M. Indeed, we observe experimentally that, for $C_s = 0.05$ M, $I(q)$ decays monotonically to zero while there is still a peak for $C_s = 0.01$ M. The domain of polymer concentration and ionization degree in which a peak of $I(q)$ is observed in the absence of salt is also consistent with the model.

As mentioned above, the behavior of the scattered intensity at the peak can be analyzed in terms of (10) and

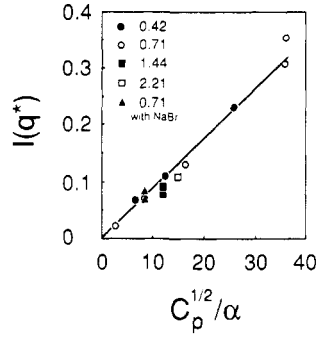

Figure 14. Variation of the peak intensity as a function of $C_p^{1/2}/\alpha$ for different polymer concentrations. The straight line corresponds to the theoretical prediction of (11).

(11). Equation 11 gives quite a nice description of the experimental results (Figure 14). On the other hand, using the representation associated with (10), i.e., $I(q)$ vs $(q^{*2} + \kappa^2)/\alpha^2$, we obtain a splitting of the data in straight lines with polymer concentration dependent slopes.

This feature reflects again the variation of the coefficient, A, with the polymer concentration. Plotting $I(q^*)$ vs $\alpha C_p^{1/2}$, we have implicitly supposed that A was a constant for all the samples, independent of the concentration. On the other hand, the quantity $(q^{*2} + \kappa^2)/\alpha^2$ contains the experimental A value that is found dependent on the polymer concentration. Thus, it seems that the theory describes correctly the concentration dependence of the peak intensity but fails on predicting the concentration dependence of the peak position. This disagreement might originate in the network nature of the systems.

We know that the unneutralized PAA gels can undergo a phase separation, since upon lowering of the pH or the temperature, they become opalescent. This corresponds to a macroscopic transition and is compatible with a very small q^* value as predicted by (9). As a matter of fact, it was shown long ago[39] that, due to hydrogen bonding, PMA and PAA chains have a poor solubility in water solutions with low pH. However, the presence of cross-links with low solubility and the unlocalized nature of the charges make these systems different from the ones considered by Borue–Erukhimovich and Joanny–Leibler in their theoretical models. It could be speculated that the separation in dense and dilute polymer regions is favored by an expulsion of the charges from the high monomer density regions, around the cross-links. On the other hand, the presence of cross-links decreases the ability of the system to rearrange. Thus, cross-links may be responsible for two competing effects, and it is difficult to predict which one will dominate. It is, however, likely that the effect of cross-link constraints should increase with the cross-linking degree.

Results presented in this paper correspond essentially to gels with the same value of the ratio R of cross-linker to monomer molar concentration ($R = 4.7 \times 10^{-3}$). In the range of polymer concentration investigated, the shear modulus varies from zero, since for $C_p = 0.42$ M there is no macroscopic gel, to 2.3×10^5 dyn/cm^2. As the increase of the shear modulus with polymer concentration is much larger than that predicted from the elasticity theory, one must conclude that it is partly due to an enhancement of the cross-linking. This is likely to be at the origin of the slight increase of the quantity A. The rearrangement of the network structure at large scales could be hindered by the cross-links, producing a quenching of a too large q^* value for the high polymer concentrations.

These points are conjectures that should be clarified in future experiments. Another important point to keep in

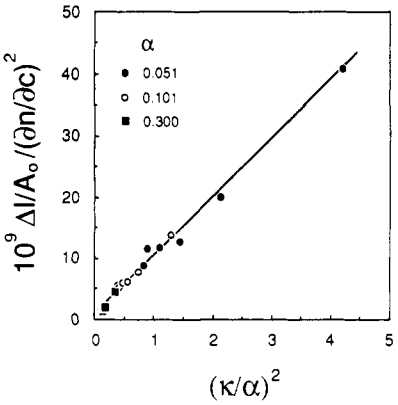

Figure 15. Plot of the data in Figure 11 as a function of $(\kappa/\alpha)^2$.

mind is that the topological architecture of these radical-type gels may be quite similar to the one proposed for poly(acrylamide)[40] or copolymerized styrene–divinylbenzene gels.[41] The influence of the topology of the network is not taken into account in the theoretical model.

The above theoretical model is successful in analyzing the light-scattering data. The intensity scattered at small q values is given by

$$S(0) = \frac{1}{4\pi l}\frac{\kappa^2}{\alpha^2} \tag{12}$$

This result could also be obtained directly from a mean-field theory of the semidilute regime that gives $S(q=0) = \upsilon_e^{-1}$.[37] The electrostatic excluded-volume, υ_e, is easily calculated by using the definition $\upsilon_e = \alpha^2 \int d^3r\ (1 - e^{-V(r)})$, where $V(r)$ is the screened electrostatic potential $V(r) = (l/r)e^{-\kappa r}$.

Figure 15 shows the same data as in Figure 10, using the representation of (12). The data gather around a straight line, which gives a strong support to the validity of (12).

The QELS experiments are more difficult to interpret. In neutral gels, the cooperative diffusion coefficient, D_c, is given by[35]

$$D_c = M/f_r \tag{13}$$

where f_r is the friction coefficient per unit volume. By use of the Kubo method, D_c can be expressed in terms of a hydrodynamic correlation length, ξ_H[42]

$$D_c = \frac{k_B T}{6\pi\eta\xi_H} \tag{14}$$

where η is the viscosity of the solvent. At swelling equilibrium, ξ_H is correlated to the mesh size of the neutral network.

In the case considered here, it would be tempting to associate ξ_H^{-1} to the position q^* of the peak observed by the SANS technique. The variations of D_c with α and C_s at a given polymer concentration are qualitatively in agreement with this assumption.[43] However, at a given $\alpha \geq 0.02$, ξ_H increases with polymer concentration, which is the opposite behavior of that of q^{*-1}. Turning back to (13), we can replace the longitudinal modulus, M, by $K_{os,e}$, since the latter is the major contribution in (6). Then in the absence of added salt, we obtain a very simple expression for D_c:

$$D_c(C_s=0) = k_B T \frac{\alpha\Phi}{f_r} \tag{15}$$

Assuming that the friction between polymer chains and solvent is the same as that in neutral gels would lead to a $\Phi^{1.5}$ or Φ^2 dependences of f_r, depending on whether the chains are swollen or Gaussian.[42] This would lead qualitatively to the observed decrease of D_c as the polymer concentration is increased. However, to account for the experimental variations of D_c with Φ and α, one must assume that f_r is function of both Φ and α. This is not surprising since the actual structure of the system as evidenced by the peak of the structure factor depends on these parameters.

V. Conclusion

The set of results reported here is broadly consistent with the model of mesophase-separation transition. In particular, the data relative to the effects of C_s and α on the peak observed in SANS experiments provide some arguments in favor of this model. The variations of q^* as the polymer concentration is changed are more difficult to understand. Some specific effects of the finite shear modulus are likely to be implied in the observed behavior.

The variations of the shear modulus with polymer concentration and cross-linking density show that the structure of the gels change in a complicated manner with these parameters. The decrease of the shear modulus as the ionization degree increases is yet to be understood.

On the other hand, the behavior of the compressional osmotic modulus can be explained in a satisfactory way by very simple considerations.

This contrasts with our understanding of the dynamical properties of these gels. To take into account the observed behavior, we must introduce into the equations a friction coefficient that has a complex dependence on polymer concentration, ionization degree, and salt concentration. More sophisticated theoretical methods should be developed to elucidate this point.

Finally there is still work to be done to understand more clearly if the cross-links and the delocalization of the electric charges influence the microphase-separation transition. It might be of interest to investigate systems with more soluble cross-linking agent and polymer chains with localized charges. Studies as a function of the temperature should allow us to observe the phase transition. They are now in progress.

Acknowledgment. We thank J. P. Cotton and L. Auvray for useful assistance during the SANS experiments and for helpful discussions about scattering experiments on polyelectrolyte systems. We also acknowledge them as well as M. Rawiso and J. Bastide for sharing their experience of SANS experiments. Our discussions with C. Strazielle were very useful in helping us to normalize the light-scattering data. We are grateful to J. F. Joanny, L. Leibler, P. Pincus, I. Rabin, E. Raphaël, and T. Witten for illuminating discussions about theoretical aspects of polyelectrolyte systems. F.I. has benefited from financial support by the Orkem Co.

References and Notes

(1) de Gennes, P.-G.; Pincus, P.; Velasco, R. M.; Brochard F. *J. Phys. (Paris)* **1976**, *37*, 1461.
(2) Odijk, T. *J. Polym. Sci., Polym. Phys. Ed.* **1977**, *15*, 477; *Macromolecules* **1979**, *12*, 688.
(3) Pfeuty, P. *J. Phys. (Paris)* **1978**, *C2*, 149.
(4) Koyama, R. *Macromolecules* **1986**, *19*, 178.

(5) Witten, T.; Pincus, P. *Europhys. Lett.* **1987**, *3*, 315.
(6) Kaji, K.; Urakawa, H.; Kanaya, T.; Kitamaru, R. *J. Phys. (Paris)* **1988**, *49*, 993.
(7) Borue, V.; Erukhimovich, I. *Macromolecules* **1988**, *21*, 3240.
(8) Joanny, J. F.; Leibler, L. *J. Phys. (Paris)* **1990**, *51*, 545.
(9) Manning, G. S. *J. Chem. Phys.* **1969**, *51*, 924, 934.
(10) Williams, C. E.; Nierlich, M.; Cotton, J. P; Jannink, G.; Boué, F.; Daoud, M.; Farnoux, B.; Picot, C.; de Gennes, P.-G.; Rinaudo, M.; Moan, M.; Wolff, C. *J. Polym. Sci., Polym. Lett. Ed.* **1979**, *17*, 379. Nierlich, M.; Williams, C. E.; Boué, F.; Cotton, J. P.; Daoud, M.; Farnoux, B.; Jannink, G.; Picot, C.; Moan, M.; Wolff, C.; Rinaudo, M.; de Gennes, P.-G. *J. Phys. (Paris)* **1979**, *40*, 701. Nierlich, M.; Boué F.; Lapp, A.; Oberthür, R. *J. Phys. (Paris)* **1985**, *46*, 649; *Colloid Polym. Sci.* **1985**, *263*, 955.
(11) Ise, N.; Okubo, T.; Kunigi, S.; Matsuoka, H.; Yamamoto, K.; Ishii, Y. *J. Chem. Phys.* **1984**, *81*, 3294.
(12) Grüner, F.; Lehmann, W. P.; Fahlbusch, H.; Weber, R. *J. Phys. A.* **1981**, *14*, L307. Koene, R.; Mandel, M. *Macromolecules* **1983**, *16*, 220; **1983**, *16*, 227; **1983**, *16*, 973. Drifford, M.; Dalbiez, J. P. *J. Phys. Chem.* **1984**, *88*, 5368; *J. Phys. (Paris), Lett.* **1985**, *46*, L311. Wang, L. X.; Yu, H. *Macromolecules* **1988**, *21*, 3498.
(13) Hayter, J.; Jannink, G.; Brochard, F.; de Gennes, P.-G. *J. Phys. (Paris) Lett.* **1980**, *41*, L451. Nallet, F.; Jannink, G.; Hayter, J. B.; Oberthür, R.; Picot, C. *J. Phys. (Paris)*, **1983**, *44*, 87. Kanaya, T.; Kaji, K.; Kitamaru, R.; Higgins, J.; Farago, B. *Macromolecules* **1989**, *22*, 1356.
(14) Koene, R.; Mandel, M. *Macromolecules* **1983**, *16*, 231.
(15) See: Wolff, C. *J. Phys. (Paris)* **1978**, *C2*, 169 and references therein.
(16) Moan, M.; Wolff, C.; Ober, R. *Polymer* **1975**, *16*, 781. Cotton, J. P.; Moan, M. *J. Phys. (Paris) Lett.* **1976**, *37*, L75. Plestil, J.; Ostanevich, Y.; Bezzabotonov, V.; Hlavata, D.; Labsky, J. *Polymer* **1986**, *27*, 839.
(17) Ise, N.; Okubo, T.; Hiragi, Y.; Kawai, H.; Hashimoto, T.; Fujimura, M.; Nakajima, A.; Hayashi, H. *J. Am. Chem. Soc.* **1979**, *101*, 5836.
(18) Noda, I.; Tsuge, T.; Nagasawa, M. *J. Phys. Chem.* **1970**, *74*, 710.
(19) Kitano, T.; Taguchi, A.; Noda, I.; Nagasawa, M. *Macromolecules* **1980**, *13*, 57.
(20) Muroga, Y.; Noda, I.; Nagasawa, M. *Macromolecules* **1985**, *18*, 1576.
(21) Dubin, P. L.; Strauss, U. P. In *Polyelectrolytes and their Applications*; Rembaum, A., Selegny, E., Eds.; D. Reidel: Dordrecht, Holland, 1975. Strauss, U. P. In *Polymers in Aqueous Media: Performance through Association*; Glass, J. E., Ed.; Advances in Chemistry Series 223; American Chemical Society: Washington, DC, 1989; p 317.
(22) Tanaka, T. *Phys. Rev. Lett.* **1978**, *40*, 280. Tanaka, T.; Fillmore, D. J.; San, S. T.; Nishio, I.; Swislov, G.; Shah, A. *Phys. Rev. Lett.* **1980**, *45*, 1636. Hirokawa, T.; Tanaka, T.; Sato, E. *Macromolecules* **1985**, *18*, 2782. Ricka, J.; Tanaka, T. *Macromolecules* **1985**, *18*, 83; **1984**, *17*, 2916.
(23) Schosseler, F.; Mallo, P.; Cretenot, C.; Candau, S. J. *J. Dispersion Sci. Technol.* **1986**, *8*, 321.
(24) Roy-Chowdhury, P.; Kale, K. M. *J. Appl. Polym. Sci.* **1970**, *14*, 2937. Tondre, C.; Zana, R. *J. Phys. Chem.* **1972**, *76*, 3451. Zana, R. *J. Polym. Sci., Polym. Phys. Ed.* **1980**, *18*, 121.
(25) As provided by the utilitary program WATWET, ILL, Grenoble, France: $(d\Sigma/d\Omega(\lambda=5.04) = 0.827\ cm^{-1}$, $(d\Sigma/d\Omega)(\lambda=8) = 0.916\ cm^{-1}$, and $(d\Sigma/d\Omega)(\lambda=14.86) = 1.101\ cm^{-1}$.
(26) Ilmain, F.; Candau, S. J. *Prog. Colloid Polym. Sci.* **1989**, *79*, 172.
(27) Ilmain, F.; Candau, S. J. *Makromol. Chem., Macromol Symp.* **1989**, *30*, 119.
(28) Candau, S. J.; Bastide, J.; Delsanti, M. *Adv. Polym. Sci.* **1982**, *44*, 27.
(29) Moussaïd, A.; Munch, J. P.; Schosseler, F.; Candau, S. J., submitted for publication in *J. Phys. (Paris)*.
(30) Dusek, K.; Prins, W. *Adv. Polym. Sci.* **1969**, *6*, 1.
(31) Daoud, M.; Cotton, J. P.; Farnoux, B.; Jannink, G.; Sarma, G.; Benoit, H.; Duplessix, R.; Picot, C.; de Gennes, P.-G. *Macromolecules* **1975**, *8*, 804. For a detailed discussion of the intermediate scattering regime, see, for example: Rawiso, M.; Duplessix, R.; Picot, C. *Macromolecules* **1987**, *20*, 630.
(32) For a discussion of partial structure factors in polyelectrolyte systems, see: Jannink, G. *Makromol. Chem., Makromol. Symp.* **1986**, *1*, 67 and references therein.
(33) Flory, P. J. *Principles of Polymer Chemistry*; Cornell University Press: Ithaca, NY, 1953.
(34) Herz, J.; Munch, J. P.; Candau, S. J. *J. Macromol. Sci. Phys. B* **1980**, *B18*, 267.
(35) Tanaka, T.; Hocker, L.; Benedek, G. B. *J. Chem. Phys.* **1973**, *53*, 5151.
(36) See for example: *Light scattering from polymer solutions*; Huglin, M. B., Ed.; Academic Press: London, 1972.
(37) Joanny, J. F.; Pincus, P. *Polymer* **1980**, *21*, 274.
(38) Alexander, S.; Chaikin, P. M.; Grant, P.; Morales, G. J.; Pincus, P.; Hone, D. *J. Chem. Phys.* **1984**, *80*, 5776.
(39) Katchalsky, A.; Eisenberg, H. *J. Polym. Sci* **1951**, *6*, 145. Kedem, O.; Katchalsky, A. *J. Polym. Sci.* **1955**, *15*, 321.
(40) Weiss, N.; Silberberg, A. *Br. Polym. J.* **1977**, *9*, 144. Weiss, N.; Van Vliet, T.; Silberberg, A. *J. Polym. Sci., Polym. Phys. Ed.* **1979**, *17*, 2229.
(41) Candau, S. J.; Young, C. Y.; Tanaka, T.; Lemaréchal, P.; Bastide, J. *J. Chem. Phys.* **1979**, *70*, 4694.
(42) de Gennes, P.-G. *Scaling Concepts in Polymer Physics*; Cornell University Press: Ithaca, NY, 1979.
(43) Ilmain, F.; Schosseler, F.; Candau, S. J. In *Molecular Basis of Polymer Networks. Proceedings in Physics*; Baumgärtner, A., Picot, C., Eds.; Springer: New York, 1989; Vol. 42, p 143.

Registry No. (Acrylic acid)(*N,N'*-methylenebis(acrylamide)) (copolymer), 30280-72-9; (acrylic acid)(*N,N'*-methylenebis(acrylamide))·*x*Na (copolymer), 54843-66-2.